

Gamma irradiation of protein-based textiles for historical collections decontamination

Maria Geba · Gabriela Lisa · Cristina Marta Ursescu ·
Angelica Olaru · Iuliana Spiridon · Ana Lacramioara Leon ·
Ioana Stanculescu

Received: 1 November 2013 / Accepted: 26 June 2014 / Published online: 23 July 2014
© Akadémiai Kiadó, Budapest, Hungary 2014

Abstract In order to investigate the effect of gamma rays on cultural heritage materials, samples of silk and wool fabrics were subjected to accelerated ageing testing and then irradiated with different gamma-ray doses: 10 and 25 kGy. In the data analysis, combining thermal analysis (TG and DTG), infrared spectroscopy (FTIR-ATR) and mechanical tests allowed us to explore the changes in physical and chemical features for silk and wool, in relationship to the radiation doses. This analytical protocol offers a way to examine the behaviour of the textiles made of wool and silk within museum collections and their response to gamma-rays irradiation treatment. An exposure to a dose of 10 kGy did not cause significant changes in the tested properties; however, higher doses initiated irreversible loss in the physical and chemical stability of protein-based fabrics. Increasing the irradiation dose above 10 kGy

has drastic effects in the loss of elasticity and the mechanical resistance of the tested yarns.

Keywords Gamma irradiation · TG · DTG · ATR-FTIR · Mechanical properties · Historical silk and wool

Introduction

Monitoring the changes induced by the environment or by material properties involved in the development of bio-deterioration processes, and their controls are challenging, ongoing tasks for the professionals working with valuable historical textile collections. In heritage conservation practice, techniques based on physical means offer alternatives to chemicals, fungicides and bactericides. Along with other pest management methods, the disinfection with ionising radiation has received increasing attention in the last decades [1–7]. This pertains to the industrial gamma ray irradiation facilities that are used mostly in the sterilisation of medical devices and for industrial application. Gamma rays of radionuclide ^{60}Co can deliver the required dose of ionising radiation for preventing micro-organisms and insect gametes from reproducing on the treated objects [8]. Irradiation has proved to be a safer method because it does not leave behind any harmful residue, and the ionising radiation does not involve any radio-activation in the historical materials [9–12].

The degradation of the organic materials contained in valuable historical objects is a very complex process. Therefore, ongoing research performed to assess the impact of gamma-ray treatments on historical materials is essential to finding the most appropriate parameters for the gamma-ray decontamination process. The effectiveness of gamma-ray decontamination is dependent upon factors like the

M. Geba (✉) · C. M. Ursescu · A. Olaru
'Moldova' National Complex of Museums Iasi, Iasi, Romania
e-mail: mariageba@yahoo.com

G. Lisa
Faculty of Chemical Engineering and Environmental Protection,
'Gh. Asachi' Technical University of Iasi, Iasi, Romania

I. Spiridon
'Petru Poni' Institute of Macromolecular Chemistry, Iasi,
Romania

A. L. Leon
Faculty of Textile-Leather Engineering and Industrial
Management, 'Gh. Asachi' Technical University of Iasi, Iasi,
Romania

I. Stanculescu
'Horia Hulubei' National Institute of Physics and Nuclear
Engineering, Magurele, Magurele, Romania

radiation dose, the dose rate for the process, the type of insect or micro-organism present, and, last but not least, on the chemical and physical properties of the organic materials within the collections [10, 11, 13].

An important step in the decision-making process of a conservation treatment for historical textiles is the ability to accurately characterise the natural polymers. In the preservation of wool or silk-made objects, the findings may reveal information about the condition of an artefact and its response to various treatments.

Due to their natural heterogeneity, wool and silk fibres are complex materials. The conformational strength and rigidity of wool keratin (up to 95 % by mass in wool) are conferred by the molecular architecture: partly crystalline, alpha-helical filaments embedded in an amorphous matrix. In wool fibres, the keratin macromolecule can take a helical conformation (α -keratin) in its native state and the unstable β -keratin conformation when the fibre is not stretched along its axis [14].

Textile silk deriving mainly from *Bombyx mori* silkworms contains extruded fibroin filaments (~ 80 mass%) and sericin (up to 20 mass%), two proteins with distinct amino acid composition that confers the difference in the secondary structure. The silk fibroin consists of two chains: (heavy) H-fibroin and (light) L-fibroin in a 1:1 ratio and linked by a disulfide bond. In the fibres, fibroin has a high degree of crystallinity due to stack β -sheets, while the family of hydrophilic proteins called sericins has a more random structure [15, 16].

The structural and morphological changes induced in natural polymers by irradiation are related to mechanical [10], structural [17] and optical properties [18], and also to thermal stability [10, 19]. For an irradiated heritage collection, the changes in polymers properties during gamma-ray exposure are influencing the evolution of the further environmental ageing. It was, therefore, considered necessary to include in this study, the hydrothermal ageing. The purpose was to mimic the degradation processes that could be induced by the temperature and relative humidity (RH) levels within the textile storage rooms, after the irradiation.

The non-irradiated silk and wool fabrics, along with the irradiated and aged samples were evaluated and compared to unaged fabrics. In order to assess the behaviour of these materials, the changes in physical, chemical features for silk and wool were determined in relationship to the radiation doses. The effects of ageing [20, 21] and exposure to doses of radiation of 10 and 25 kGy on the thermal, spectral and mechanical properties of textiles were explored using thermal analysis (TG/DTG), infrared spectroscopy (FTIR-ATR) and mechanical tests. This analytical protocol, as a combination of previous studies concerning the degradation of protein-based artefacts [19–28] offered a

way to examine the behaviour of textiles made from wool and silk within museum collections, when subjected to gamma-rays irradiation treatment.

Experimental

Materials

The experiments were performed with a wool fabric (referred to as W) supplied by a traditional manufacturer (16×20 threads cm^{-1}) and a pure silk tissue (referred to as S) (9 g mq^{-1} average surface mass) supplied by Bresciani SRL, Italy.

Methods

Accelerated ageing

The artificial ageing was simulating the presence of two main natural ageing factors: heat and relative humidity. The hydrothermal ageing conditions were set at $40 \text{ }^\circ\text{C}$, 65 % RH in a lab chamber (Angelantoni Ind., Italy), with samples removed at zero (and labelled W0 and S0), 24 (samples labelled W24 and S24), 48 (for samples W48 and S48) and 120 h (for samples W120 and S120). The behaviour of the aged samples of wool and silk was compared to that of the unaged samples W0 and S0.

Gamma rays irradiation

Irradiation was performed on the reference samples W0, S0 and on the samples aged for 120 h W120, S120 in a ^{60}Co irradiation unit (SVST Co-60/B type) at IRASM-Magurele facility, Romania. The total radiation doses were 10 and 25 kGy, with a dose uniformity ratio $D_{\text{max}}/D_{\text{min}} = 1.14$. The irradiated samples were labelled according to ageing and irradiation doses: W0_10, W120_10, W0_25, W120_25 and S0_10, S120_10, S0_25, S120_25.

TG/DTG analysis

In order to describe the thermal degradation of the textiles, analysis of silk and wool samples (2–6 mg) was carried out using a DSC-30 instrument (Mettler Toledo).

The quantification of thermal degradation through thermogravimetric analysis was performed under air and nitrogen environments, using a 20 mL min^{-1} flow rate, over the temperature range of $25\text{--}600 \text{ }^\circ\text{C}$. The mass loss of the two protein-based samples was measured with a constant rate of temperature increase of $10 \text{ }^\circ\text{C min}^{-1}$, as a function of temperature and time.

Fig. 1 TG and DTG curves of the tested wool samples in the environments of nitrogen and air

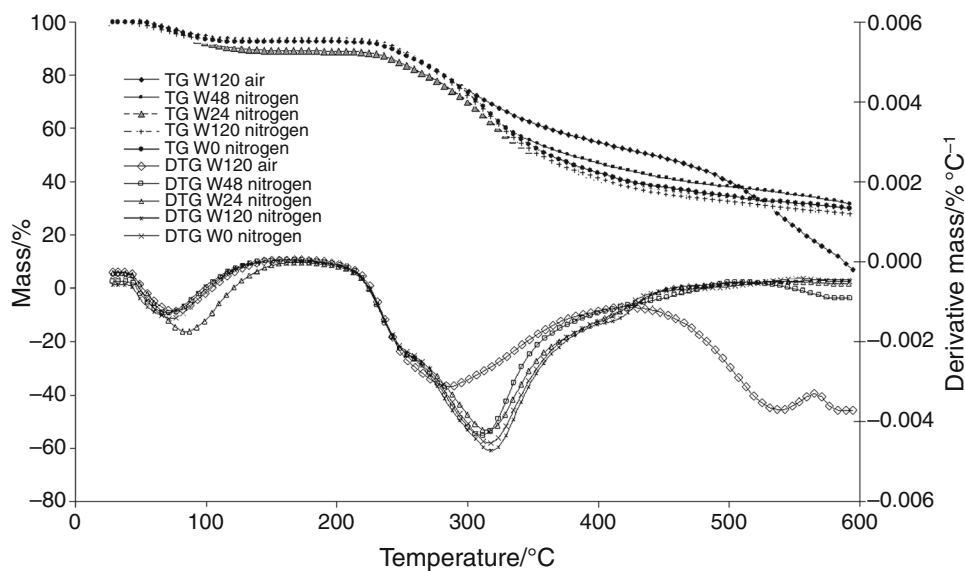
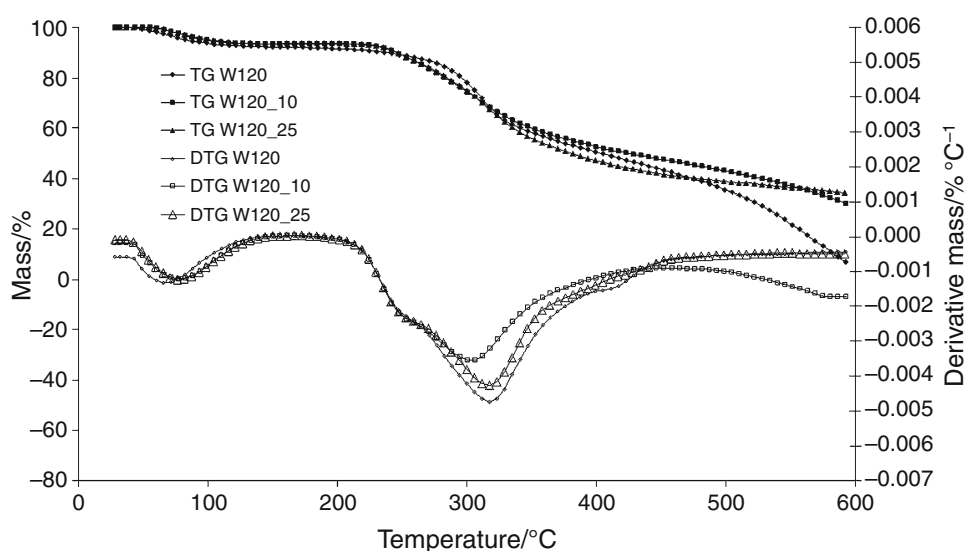


Fig. 2 TG and DTG curves in nitrogen of the aged sample of wool (W120), the sample irradiated at 10 kGy (W120_10) and after a 25 kGy irradiation treatment (W120_25)



Attenuated total reflectance (ATR)-FTIR

For the above mentioned samples, Fourier transform infrared spectra were collected on a Vertex 70 model spectrometer (Bruker, Germany) equipped with a ZnSe ATR accessory, in the wavenumber range of $4,000\text{--}600\text{ cm}^{-1}$, at a resolution of 2 cm^{-1} , with 64 consecutive scans.

Mechanical measurements

After the hydrothermal ageing treatment, some yarns were extracted from the fabrics, and the main tensile properties, the breaking force (N) and relative elongation or deformation to rupture (%), were measured using a TINIUS

OLSEN H5KT dynamometer, according to ISO 2062 standard method. The average values were calculated from nine measurements.

Results and discussion

TG and DTG

The plots of the thermogravimetric (TG) and derivative thermogravimetric (DTG) curves in nitrogen environment for the wool samples W0, W24, W48 and W120 are shown in Fig. 1. This figure also shows TG/DTG curves in air for sample W120. The influence of the two radiation doses on

Table 1 Thermogravimetric characteristics of the tested wool yarns in nitrogen atmosphere

Nitrogen						
Sample	Degradation step	$T_{onset}/^{\circ}\text{C}$	$T_{peak}/^{\circ}\text{C}$	$T_{endset}/^{\circ}\text{C}$	Mass loss/%	Residue
W0	I	51.30	72.14	108.48	7.93	29.44
	II	231.57	317.29	437.77	62.63	
W24	I	63.38	84.36	123.33	11.11	28.21
	II	233.07	316.70	439.83	60.68	
W48	I	48.83	69.99	113.43	7.61	30.83
	II	233.11	312.38	434.49	61.56	
W120	I	50.69	66.56	98.07	7.24	27.89
	II	234.05	320.32	427.23	64.90	
W120_10	I	54.83	78.28	119.16	7.22	29.05
	II	231.82	303.81	412.22	63.73	
W120_25	I	53.92	77.84	119.96	7.16	33.56
	II	229.58	317.11	432.46	59.28	

T_{onset} the temperature where thermal degradation starts, T_{peak} the temperature at the maximum thermal degradation, T_{endset} the temperature where the degradation process ends

Table 2 Thermogravimetric characteristics of the tested wool yarns in air atmosphere

Air						
Sample	Degradation step	$T_{onset}/^{\circ}\text{C}$	$T_{peak}/^{\circ}\text{C}$	$T_{endset}/^{\circ}\text{C}$	Mass loss/%	Residue
W0	I	50.12	76.14	123.18	2.91	5.41
	II	235.44	284.79	376.58	42.84	
	III	468.59	532.22	–	48.84	
W120	I	55.40	74.59	111.72	7.21	6.06
	II	236.42	283.70	360.67	40.23	
	III	494.16	536.88	–	46.5	

T_{onset} the temperature where thermal degradation starts, T_{peak} the temperature at the maximum thermal degradation, T_{endset} the temperature where the degradation process ends

the aged sample W120 is shown in Fig. 2. Experimental data for TG measurements under nitrogen for the above mentioned samples of wool are shown in Table 1, whereas Table 2 contains the results for the experiments run in air.

As shown in Table 1 and reflected by Figs. 1 and 2, the onset of degradation is at 230–234 °C with minor changes induced by accelerated ageing or radiation doses. The level of humidity in the samples is in the range of 7–11 %. The char residue at 600 °C is 30 % by mass, under these testing conditions. In the case of the proteins, strong hydrogen bonded structures are reflected in the stability to high degradation temperatures, with increased amounts of tar or char residue. The effect of air atmosphere on the thermal stability of the wool samples is shown in Table 2.

The thermal decomposition reveals three steps in the degradation, and the process seems to be ongoing as the temperature exceeds 600 °C (see Fig. 1). The residuary mass is, as expected, lower as compared to an inert

atmosphere, and this can be attributed to the fact that the formed residue is further oxidised by oxygen. As shown in Fig. 2 and Table 1, gamma-ray exposure to a dose value lower than 10 kGy does not have a great influence on the thermal stability of the wool fibres submitted to hydrothermal ageing for 120 h (W120).

For the tested silk samples, TG and DTG curves for the experiments run under nitrogen and air are highlighted in Fig. 3. The TG and DTG plots for the irradiated samples are illustrated, as labelled in Fig. 4. The resulting data on the thermogravimetric characteristics are shown in Tables 3 and 4.

Both in nitrogen and air atmosphere, the thermal stability of the aged samples is slightly diminishing (Tables 1, 2). It is worth noting that the value of T_{peak} in the main degradation step is around 316 °C for the samples of aged silk S120. Figure 4 shows the TG and DTG curves of the sample aged for 120 h in hydrothermal conditions (S120),

Fig. 3 TG and DTG curves of the tested silk samples in the environments of nitrogen and air

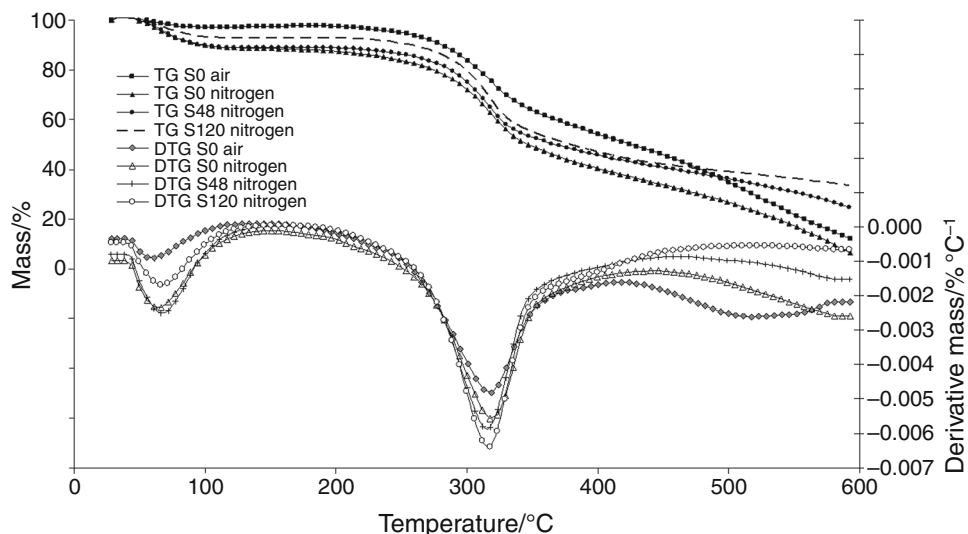


Fig. 4 TG and DTG curves in nitrogen of the aged sample of silk (S120), the sample irradiated at 10 kGy (S120_10) and after a 25 kGy irradiation treatment (S120_25)

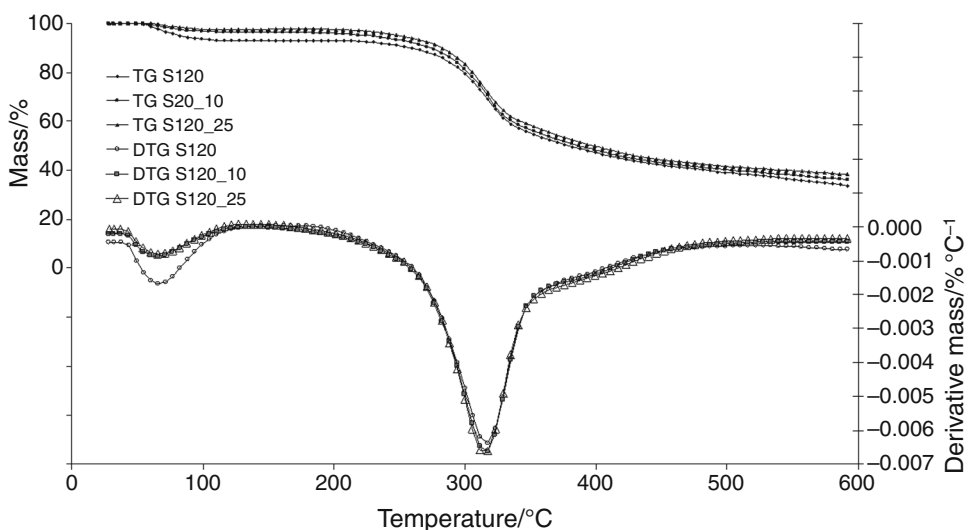


Table 3 Thermogravimetric characteristics of the tested silk yarns in air atmosphere

Air						
Sample	Degradation step	$T_{onset}/^{\circ}C$	$T_{peak}/^{\circ}C$	$T_{endset}/^{\circ}C$	Mass loss/%	Residue
S0	I	45.22	59.05	97.01	3.87	9.82
	II	266.86	318.61	360.08	43.79	
	III	460.26	522.38	–	42.52	
S120	I	46.11	62.22	102.18	10.53	8.46
	II	265.34	316.41	353.22	38.24	
	III	419.22	498.82	–	42.77	

T_{onset} the temperature where thermal degradation starts, T_{peak} the temperature at the maximum thermal degradation, T_{endset} the temperature where the degradation process ends

Table 4 Thermogravimetric characteristics of the tested silk yarns in nitrogen atmosphere

Nitrogen						
Sample	Degradation step	$T_{onset}/^{\circ}\text{C}$	$T_{peak}/^{\circ}\text{C}$	$T_{endset}/^{\circ}\text{C}$	Mass loss/%	Residue
S0	I	45.62	62.45	103.50	12.97	4.48
	II	273.53	319.63	424.34	82.55	
S24	I	41.47	126.97	156.94	10.21	30.78
	II	279.51	318.85	426.20	59.01	
S48	I	45.83	66.64	91.98	12.49	23.16
	II	276.44	316.45	422.37	64.35	
S120	I	47.62	66.74	93.01	8.02	32.49
	II	266.56	316.74	425.45	59.49	
S120_10	I	47.59	63.35	95.27	4.24	35.38
	II	264.82	316.21	429.13	60.38	
S120_25	I	45.96	66.58	98.40	3.75	36.83
	II	264.77	315.00	426.30	59.42	

T_{onset} the temperature where thermal degradation starts, T_{peak} the temperature at the maximum thermal degradation, T_{endset} the temperature where the degradation process ends

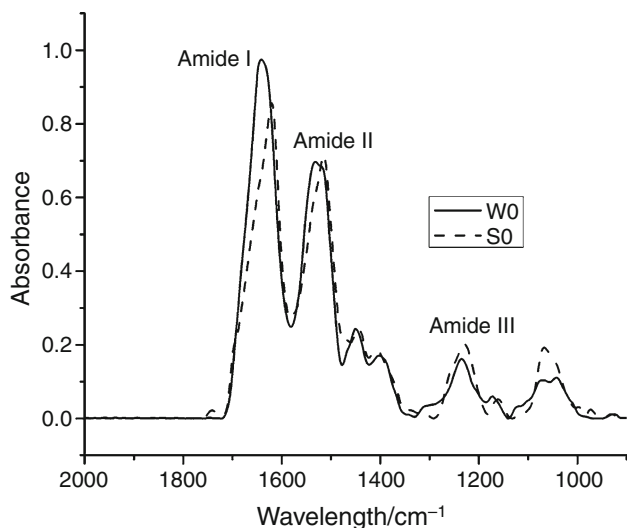


Fig. 5 ATR spectra of protein-based textiles: reference wool (W0) and reference silk (S0)

irradiated at 10 and 25 kGy. As the radiation dose increases, the endothermic peak temperature of silk sample slightly decreases [30], but the absorbed doses led to insignificant changes in the thermal stability for the aged sample.

Attenuated total reflectance (ATR)-FTIR spectroscopy

FTIR spectroscopy provides information about the secondary structure content and changes of the textile proteins, that are closely related to the physical and chemical

properties of silk and wool fibres. The more informative infrared bands to analyze proteins are the characteristic absorption bands assigned to the peptide bonds ($-\text{CONH}-$), bands known as amide I, II and III. Amide I absorption is associated with the $\text{C}=\text{O}$ stretching vibrations, and it occurs in the range of $1,700-1,600\text{ cm}^{-1}$. Amide II vibration leads to the $\text{N}-\text{H}$ bending and $\text{C}-\text{N}$ stretching vibration, in the $1,540-1,520\text{ cm}^{-1}$ range. Both the Amide I and Amide II bands are sensitive to the secondary structure content of a protein, because $\text{C}=\text{O}$ and the $\text{N}-\text{H}$ bonds are involved in the hydrogen bond between the different elements of secondary structure. Amide III vibration is associated to the combination of $\text{N}-\text{H}$ bending and CN stretching of the peptide group and occurs in the range of $1,220-1,300\text{ cm}^{-1}$ [24, 26–29].

In Fig. 5, the fingerprint region in the spectral range $1,700-900\text{ cm}^{-1}$ is plotted for the tested protein-based fibres. The ATR-FTIR spectra of the unaged wool showed the characteristic bands of keratin at around $1,641\text{ cm}^{-1}$ for amide I, $1,533\text{ cm}^{-1}$ for amide II and $1,234\text{ cm}^{-1}$ for amide III. The spectra of silk fibroin in the model textiles yarns contain characteristic absorption bands assigned to the peptide bonds ($-\text{CONH}-$), namely bands of amide I at $1,620\text{ cm}^{-1}$, $1,514\text{ cm}^{-1}$ for amide II, and around $1,231\text{ cm}^{-1}$ for amide III.

For the textile fibres submitted to hydrothermal ageing for 120 h and irradiated with gamma-ray doses of 10 and 25 kGy, this study uses as markers of alteration in protein-based fibres (silk fibroin and wool keratin) the following data indicated by the literature: the ratio of amide I and II bands; the separation between amide I and II bands, and $I_{\text{Amide III}}/I_{1,450\text{ cm}^{-1}}$ the ratio of Amide III band and the band

Table 5 Main spectral changes in the ATR-FTIR spectra of wool keratin samples

Sample	W0	W0_10	W0_25	W120	W120_10	W120_25
$I_{\text{Amide I}}/I_{\text{Amide II}}$	1.37	1.29	1.23	1.40	1.32	1.27
$I_{\text{Amide III}}/I_{1450}$	0.73	0.84	0.73	0.67	0.92	0.64
$\Delta\nu = \nu_{\text{Amide I}} - \nu_{\text{Amide II}}$	108	104	101	110	107	101

Table 6 Main spectral changes in the ATR-FTIR spectra of silk fibroin samples

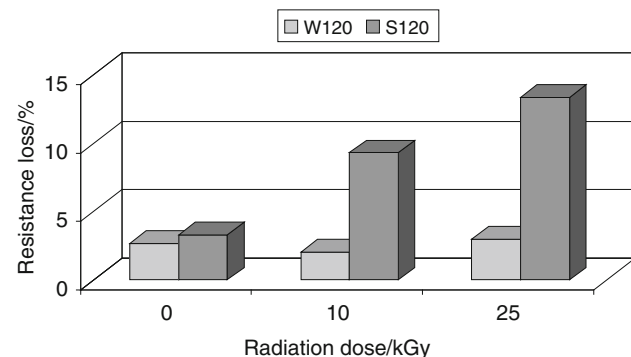
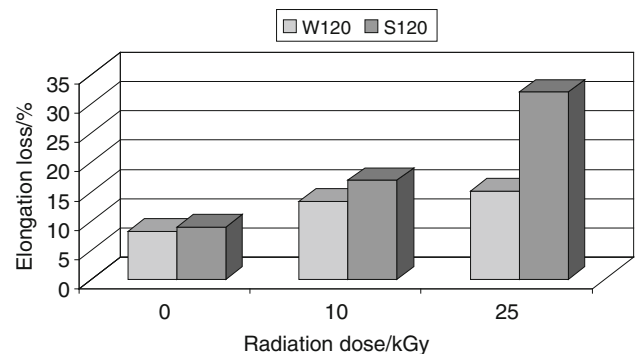
Sample	S0	S0_10	S0_25	S120	S120_10	S120_25
$I_{\text{Amide I}}/I_{\text{Amide II}}$	1.20	1.13	1.12	1.17	1.33	1.13
$I_{\text{Amide III}}/I_{1450}$	0.95	0.84	0.75	0.82	0.82	0.76
$\Delta\nu = \nu_{\text{Amide I}} - \nu_{\text{Amide II}}$	106	104	106	106	107	106

Table 7 Tensile properties of model wool subjected to hydrothermal ageing followed by gamma-ray exposure

Wool yarns	Breaking force/N		Relative elongation/%	
	0	120	0	120
Ageing/h				
Dose/kGy				
0	3.83	3.63	14.23	12.65
10	3.31	3.24	15.01	13.78
25	3.57	3.43	15.09	13.01

Table 8 Tensile properties of model silk subjected to hydrothermal ageing followed by gamma-ray exposure

Silk yarns	Breaking force/N		Relative elongation/%	
	0	120	0	120
Ageing/h				
Dose/kGy				
0	0.34	0.32	10.13	8.88
10	0.34	0.30	12.37	9.91
25	0.37	0.29	11.09	7.10

**Fig. 6** Comparisons of the resistance loss indicating the extent of changes in the 120 h aged wool and silk samples, after exposure to increasing radiation doses**Fig. 7** Comparisons of the elongation loss (%) indicating the extent of changes in the 120 h aged wool and silk samples, after exposure to increasing radiation doses

intensity at $1,450\text{ cm}^{-1}$, corresponding to CH_2 vibrations (Tables 5, 6) [24–27, 31, 32].

An increase in the OH band at $1,650\text{ cm}^{-1}$ would result in an increase in the absorption intensity or height of the amide I band. Thus, the increase of the amide I/amide II ratio can be associated with hydrolysis of the polypeptide chains; the increase in the distance between the two amidic structures (amide I–amide II) indicates a denaturation of the amide structure, while $I_{\text{Amide III}}/I_{1,450\text{ cm}^{-1}}$ may indicate the denaturation of the helix. Spectral changes in the amide I carbonyl stretching region can be related to changes in the triple helical structure of the natural polymers [24, 26, 31, 32].

The denaturation of the helix is more evident when considering changes in the ratio $I_{\text{Amide III}}/I_{1450}$ for the samples subjected both to ageing and irradiation treatments (up to 10 % for the silk fibroin and up to 24 % for the wool). There was no evidence of oxidative processes during the treatments. These facts suggested that heat, humidity and gamma-ray exposure promoted deterioration on fibroin and keratin at the triple helical structure level.

Mechanical changes

Tables 7 and 8 summarise the mean values for the breaking force (N) and relative elongation (%) for the irradiated wool and silk fibres. The axial tension tests performed along the longitudinal direction revealed changes in tensile properties due to the hydrothermal ageing and to the exposure to 10 and 25 kGy gamma-ray radiation doses.

The tested samples showed a tendency towards reduced breaking force and elongation at break due to irradiation, as shown in Figs. 6 and 7. The diagrams in Figs. 6 and 7 illustrate the losses of resistance and elongation at rupture for the samples submitted to 120 h of ageing after exposure to increasing radiation doses. They are based on the calculated differences in comparison to the standard samples (0 h ageing).

The comparative analysis points out the fact that both types of protein yarn that were subjected to axial (longitudinal) traction have lost from their initial values of resistance and elongation, after having been subjected to accelerated ageing for 120 h [25] and then irradiated. The silk yarns are more sensitive to ageing [27] and irradiation [30] than the wool. The silk yarns aged for 120 h show a bigger resistance loss (6.55 %) and elongation loss (12 %) compared to the wool yarns that lose 5 % in resistance and 11 % in elongation (see Fig. 7). When irradiation processes are performed, the differences between the two types of protein-based yarns are visible. At an irradiation dose of 10 kGy, the silk yarns lose 11 % of their ultimate strength compared to the 2 % loss of the wool yarns. Increasing the irradiation dose above 10 kGy has more drastic effects in the loss of elasticity and the mechanical resistance of the tested yarns. The irradiation process combined with the ageing almost doubles the elongation loss of the silk yarns compared to the wool ones—respectively 18.35 % versus 9.26 %. Anyway, the experiments at doses usually applied in sterilisation treatments (25 kGy) were conducted in order to overestimate the induced degradation at 10 kGy and to validate the need for further tests at lower doses (2–10 kGy). With regard to the variation of the elongation at rupture, the yarns aged for 120 h and un-irradiated show similar losses: 12.34 % for the silk yarns and 11.09 % for the wool yarns. Based on the tensile tests, irradiation treatment should be applied at doses lower than 10 kGy.

Conclusions

Subjecting the silk and wool yarns to hydrothermal ageing, followed by varying conditions of irradiation led to the differences between untreated and treated materials to become increasingly apparent. The pattern in the ageing degradation of the tested textiles depends not only on the

protein type content, namely keratin and fibroin, but also on the ageing procedure. Artificial ageing produced minor alterations in the physical–chemical properties of tested wool and silk threads.

In artificially aged protein-based fibres, smaller ^{60}Co doses (up to 10 kGy) did not cause significant changes in the thermal degradation behaviour or conformational changes, compared with the un-irradiated fibres. Both wool and silk showed a trend towards reduced tensile properties due to irradiation, the process evolving more slowly for the wool. The behaviour at the dose usually applied in sterilisation treatments (25 kGy) was tested during experiments in order to overestimate the induced degradation at 10 kGy and to validate the need for further tests at lower doses (2–10 kGy).

The combination of thermal analysis (TG and DTG), infrared spectroscopy (FTIR-ATR) and mechanical tests yielded data that helped determine the most appropriate range for the gamma-ray doses used in the decontamination process, without affecting the properties of textile collections. Based on this analytical protocol for investigating the degradation behaviour of silk and wool textiles, irradiation treatment should be applied at doses lower than 10 kGy.

Acknowledgements Part of this work was supported by the Romanian Executive Agency for Higher Education, Research, Development and Innovation Funding (UEFISCDI) through the project TEXLECONS, PN-II-PT-PCCA-2011-3-1742, contract no. 213/2012.

References

1. Belyakova LA. Gamma radiation as a means of disinfection of books against spores of mould fungi. *Mikrobiologiya*. 1960;29:762–5.
2. de Tassigny C, Brouqui M. Adaptation a la desinfection de la momie de Ramses II du procede de radio-sterilisation gamma, Preprints of ICOM Committee for Conservation 5th Triennial Meeting, 1–8 Oct., 1978, Zagreb, International Council of Museums, Paris.
3. Magaúda G. The recovery of biodeteriorated books and archive documents through gamma radiation: some considerations on the results achieved. *J Cult Herit*. 2004;5:113–8.
4. da Silva M, Moraes AML, Nishikwa MM, Gahi MJA, da Alencar MA, Brandão LE. Inactivation of fungi from deteriorated paper materials by radiation. *Int Biodeterior Biodegrad*. 2006;2006(57):163–7.
5. Moise IV, Virgolici M, Negut CD, Manea M, Alexandru M, Trandafir L, Zorila FL, Talasman CM, Manea D, Nisipeanu S, Haiducu M, Balan Z. *Radiat Phys Chem*. 2012;81:1045–50.
6. Negut CD, Bercu V, Dului OGH. Defects induced by gamma irradiation in historical pigments. *J Cult Herit*. 2012;13:397–403.
7. Manea MM, Negut CD, Stanculescu IR, Ponta CC. Irradiation effects on canvas oil painting: spectroscopic observations. *Radiat Phys Chem*. 2012;81:1595–9.
8. Farkas J. Irradiation for better foods. *Trends Food Sci Technol*. 2006;17(4):148–52.

9. Adamo M, Brizzi M, Magaudda G, Martinelli G, Plossi-Zappala M, Rocchetti F, Savagnone F. Gamma radiation treatment of paper in different environmental conditions: chemical, physical and Microbiological analysis. *Restaurator*. 2001;22:107–31.
10. Bratu E, Moise IV, Cutrubinis M, Negut DC, Virgolici M. Archives decontamination by gamma irradiation. *Nukleonika*. 2009;54(2):77–84.
11. Katusin-Razem B, Razem D, Braun M. Irradiation treatment for the protection and conservation of cultural heritage artefacts in Croatia. *Radiat Phys Chem*. 2009;78:729–31.
12. Rochetti F, Adamo M, Magaudda G. Fastness of printing inks subjected to gamma-ray irradiation and accelerated ageing. *Restaurator*. 2002;23:15–26.
13. Mitran A, Ponta C, Danis A. Traitement antimicrobien des films cinématographiques au moyen du rayonnement gamma. In: *La Conservation à l'ère du Numérique*. In: Proceedings of the 4th international days of research of the association for scientific research on graphic arts (ARSAG), Paris, 27–30 May 2002. Association pour la recherche scientifique sur les arts graphiques (ARSAG), Paris, France, 2002;235–248.
14. Vasconcelos G, Freddi A, Cavaco-Paulo. Biodegradable materials based on silk fibroin and keratin. *Biomacromolecules*. 2008;9:1299–305.
15. Hakimi O, Knight D, Vollrath F, Vadgama P. Spider and mulberry silkworm silks as compatible biomaterials. *Compos B*. 2007;38(3):324–37.
16. Cardamone JM, Tunick MH, Onwulata CI. Keratin sponge/hydrogel part 1. fabrication and characterization. *Text Res J*. 2013;83(7):661–70.
17. Geba M, Vlad AM, Ciovica S. Gamma irradiation for the preservation of historical papers: a critical evaluation. *Cellul Chem Technol*. 2008;42:97–102.
18. Adamo M, Magaudda G, Omarini S. Biological measurement of damage occurring to the inner structure of paper after gamma irradiation. *Restaurator*. 2007;28:39–46.
19. Severiano LC, Rocco Lahr FA, Bardi MAG, Machado LDB. Evaluation of the effects of gamma radiation on thermal properties of wood species used in Brazilian artistic and cultural heritage. *Therm Anal Calorim*. 2011;106:783–92.
20. Mei-Ying L, Yang Z, Tong T, Xiao-Hui H, Bei-Song F, Shun-Qing W, Xin-Yu S, Hua T. Study of the degradation mechanism of Chinese historic silk (*Bombyx mori*) for the purpose of conservation. *Polym Degrad Stab*. 2013;98(3):727–35.
21. Odlyha M. Introduction to the preservation of cultural heritage. *J Therm Anal Calorim*. 2011;104(20):399–403.
22. Badea E, Miu L, Budrugaec P, Giurginca M, Mašić A, Badea N, Della Gatta G. Study of deterioration of historical parchments by various thermal analysis techniques complemented by SEM, FTIR, UV-Vis-NIR and unilateral NMR investigations. *J Therm Anal Calorim*. 2008;91:17–27.
23. Badea E, Della Gatta G, Budrugaec P. Characterisation and evaluation of the environmental impact on historical parchments by differential scanning calorimetry. *J Therm Anal Calorim*. 2011;104(2):495–506.
24. Zhang XM, Wyeth P. Using FTIR spectroscopy to detect sericin on historic silk. *Sci China Ser B*. 2010;53(3):626–31.
25. Tonin C, Aluigi A, Bianchetto Songia M, D'Arrigo C, Mormino M, Vineis C. Thermoanalytical characterisation of modified keratin fibres. *J Therm Anal Calorim*. 2004;77(3):987–96.
26. Garside P, Wyeth P. Crystallinity and degradation of silk: correlations between analytical signatures and physical condition on ageing. *Appl Phys A*. 2007;89(4):871–6.
27. Zhang X, Wyeth P. Performance measurement of sericin-coated silks during aging. *Sci China Ser B*. 2011;54(6):1011–6.
28. Wojciechowska E, Wlochowicz A, Weselucha-Birczynska A. Application of Fourier-transform infrared and Raman spectroscopy to study degradation of the wool fiber keratin. *J Mol Struct*. 1999;511(1–3):307–18.
29. Boulet-Audet M, Lefèvre Th, Buffeteau Th, Pézolet M. Attenuated total reflection infrared spectroscopy: an efficient technique to quantitatively determine the orientation and conformation of proteins in single silk fibers. *Appl Spectrosc*. 2008;62(9):956–62.
30. Yanagi Y, Kondo Y, Hirabayashi K. Deterioration of silk fabrics and their crystallinity. *Text Res J*. 2000;70(10):871–5.
31. Cucos A, Budrugaec P, Mitrea S, Hajdu C. The influence of sodium chloride on the melting temperature of collagen crystalline region in parchments. *J Therm Anal Calorim*. 2013;111(1):467–73.
32. Marincas O, Giurginca M. Conservation-restoration of textile materials from romanian medieval art collections i. Spectral characteristics of the naturally aged silk, *Revista de Chimie*. 2009;60(1):9–14.